Colloids and Surfaces A: Physicochemical and Engineering Aspects 726 (2025) 138080

Contents lists available at ScienceDirect

Colloids and Surfaces A: Physicochemical and Engineering Aspects

journal homepage: www.elsevier.com/locate/colsurfa

Owens-Wendt method as a tool to evaluate polarity of polymer-polymer aqueous two-phase systems

Alexandre M.S. Jorge [a], João A.P. Coutinho [b], Jorge F.B. Pereira [a,*]

[a] Department of Chemical Engineering, CERES, FCTUC, University of Coimbra, Rua Sílvio Lima, Pólo II - Pinhal de Marrocos, Coimbra 3030-790, Portugal

[b] CICECO – Aveiro Institute of Materials, University of Aveiro, Department of Chemistry, Campus Universitário de Santiago, Aveiro 3810-193, Portugal

HIGHLIGHTS

- The polarity of PEG600/PPG400ATPS was assessed through the Owens-Wendt method.
- PEG increased system's polarity via H-bonding with H_2O; PPG showed weaker H_2O affinity.
- Phase separation occurred when polarity contrast between PEG600/H_2O clusters and PPG400 exceeded a critical threshold.
- Increased polymer content lowered polarity gap, yielding a new monophasic regime at D/P > 0.50.
- Owens-Wendt method is a reliable and sensitive tool for assessing polarity in ATPS.

GRAPHICAL ABSTRACT

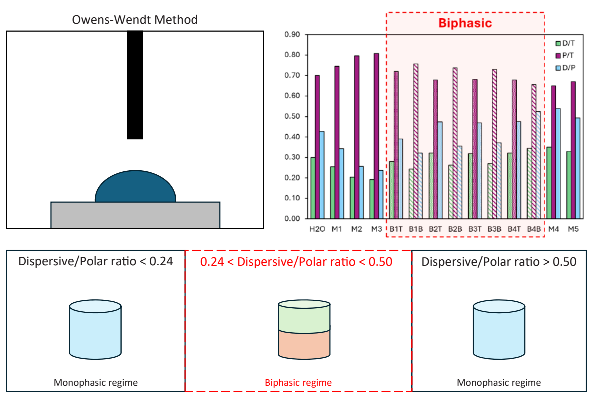

ARTICLE INFO

Keywords:
Aqueous Two-Phase Systems
Contact Angle
Polarity
Owens-Wendt method
Surface Energy

ABSTRACT

Phase separation in polymer-polymer aqueous two-phase systems (ATPS) is driven by polarity differences from intermolecular interactions. In this study, we applied the Owens-Wendt method to evaluate polarity changes during the formation of polymer-polymer ATPS and to characterize their individual phases. Surface energy contributions of polytetrafluoroethylene (PTFE), polyethylene terephthalate (PET), high-density polyethylene (PE), polyurethane (PU), polyamide (PA), polyvinyl chloride (PVC), and glass were determined using water (H_2O) and dimethyl sulfoxide (DMSO) as reference liquids. Afterward, the polarity of both binary polymer/H_2O and the ternary PEG600/PPG400/H_2O systems were determined. Binary polymer/H_2O mixtures of PEG600 and PPG400 exhibited distinct behaviours due to the additional methyl group in PPG400, which increases its hydrophobicity relative to PEG600. As polymer concentration increased, the overall polarity of the mixtures decreased for both systems. In PEG600/H_2O mixtures, dispersive forces increased as hydrogen bonding between polymer and water molecules diminished. Conversely, PPG400/H_2O mixtures displayed largely constant dispersive contributions, likely due to steric-driven self-aggregation of PPG400 molecules and consistent hydrogen bonding with water across all polymer concentrations. In ternary mixtures, the contact angle measurements indicated that PEG600 increases the mixtures' polarity through strong hydrogen bonding with H_2O, whereas PPG400 exhibits lower polarity and weaker interactions with H_2O molecules. Phase separation was

* Corresponding author.
E-mail address: jfbpereira@eq.uc.pt (J.F.B. Pereira).

https://doi.org/10.1016/j.colsurfa.2025.138080
Received 19 June 2025; Received in revised form 1 August 2025; Accepted 16 August 2025
Available online 18 August 2025
0927-7757/

attributed to the formation and disruption of hydrogen bonds within PEG600/H_2O clusters, occurring when the polarity contrast between these clusters and PPG400 exceeded a critical threshold (Dispersive/Polar (D/P) ratio < 0.24). As polymer concentration increased and H_2O content decreased, polarity differences diminished, leading to the reestablishment of a monophasic system due to stronger apolar intermolecular interactions between polymer molecules (D/P ratio > 0.50). These findings establish the Owens-Wendt method as a reliable tool for assessing ATPS polarity, even in systems with ultralow interfacial tensions. This study opens new avenues for correlating phase polarity with ATPS formation and solute partitioning, providing a novel approach to better understand and optimize liquid-liquid extraction processes, and supporting the future development of tailored ATPS-based extraction approaches with enhanced efficiency and selectivity.

1. Introduction

Aqueous Two-Phase Systems (ATPS), also known as Aqueous Biphasic Systems (ABS), have been widely employed for the separation, extraction, and purification of various (bio)molecules, as well as for understanding the thermodynamics of Liquid-Liquid Phase Separation (LLPS) [1,2]. Their widespread study began in 1958, when Albertsson *et al.* [3] first demonstrated the formation polymer/polymer ATPS by combining water, methylcellulose, and dextran and their effectiveness in selectively partitioning proteins [1]. The high-water content of both coexisting phases, coupled with enhanced biocompatibility of polymer/polymer ATPS, made these systems the preferred choice for studies focused on separation and purification of biomolecules in the later decades [2,4,5].

Despite extensive research on these liquid-liquid extraction (LLE) systems, the fundamental intermolecular mechanisms and forces driving their formation and solute partitioning behaviour remain poorly understood [6–10]. Thermodynamically, ATPS formation occurs when the Gibbs free energy change (ΔG) of the system becomes negative, favouring phase separation (*i.e.*, indicating that phase separation is thermodynamically favourable) [1]. The phase separation process and the partitioning behaviour of solutes depend on both the chemical nature of the analytes and the physicochemical properties of the ATPS' phases [11,12]. Among these, phase polarity plays a critical role, as it strongly influences the interfacial tension, and to preferential partition of solutes between the phases based on their relative hydrophobicity/hydrophilicity [11,13]. The differences in the solvent properties, and consequently the relative phases' polarity, are key to the selective partitioning of target solutes [7,11,14]. Therefore, accurate determination of phase polarity is essential for understanding and optimizing ATPS behaviour, achieving specific extraction and purification goals [10,15,16].

The role of phase polarity has been extensively studied for different types of ATPS. In 2012, Freire *et al.* [17] reported that the phases' polarities of polyethylene glycol (PEG)/ionic liquid (IL) ATPS could be tuned through the selection of the polymer's molecular weight or the chemical structure of the IL ions, allowing for control over phase separation and partition behaviour. ATPS with greater polarity differences between the phases in equilibrium tend to exhibit more efficient phase separation dynamics. The migration of target analytes between phases is influenced by the analytes' polarity, size, and charge, as well as the polarity of ATPS coexisting phases [14,17]. Pereira *et al.* [18] used three dyes with varying polarities to evaluate the relative hydrophobicity/hydrophilicity of different ATPS, demonstrating that understanding ATPS polarity differences is essential for fine-tuning these systems to selectively separate compounds with distinct or even similar properties but with differences on their own relative polarities. Other methods for the indirect determination of ATPS phase polarities include the use of hydrophobicity probes [19,20], the evaluation of hydrophobic properties in aqueous polymeric biphasic systems compared to water–organic solvent systems [21], or the use of computational tools to elucidate interactions between ATPS constituents and water [22].

To explore the molecular interactions responsible for macroscopic phase segregation and solute partition in ATPS, we have been studying ATPS composed of polyethylene glycol with a molecular weight of 600 g/mol (PEG600), polypropylene glycol with a molecular weight of 400 g/mol (PPG400) and H_2O. In a previous work we showed that phase separation in these systems is primarily driven by differences in hydrogen bonding behaviour between the polymers and H_2O [6]. By combining experimental data with molecular dynamics simulations, we demonstrated that the relative weaker interactions of PPG400 with H_2O, attributable to its more hydrophobic character arising from an additional $–CH_3$ group per monomer, led to its self-aggregation and promoted phase separation [6]. These findings confirmed that the formation of polymer/polymer ATPS depends on the differential affinity of each polymer for the solvent (H_2O) [8,9,23]. Although earlier studies have proposed indirect methods for determining ATPS polarities and empirical correlations to explain the phase separation behaviours in ATPS [7,8,24], experimental validation concerning the changes in heteromolecular interactions and phases polarities remains limited, particularly if analysed within a perspective of the ATPS formation and partitioning mechanisms.

The Owens-Wendt method (also known as Owens-Wendt-Rabel-Kaelble or OWRK model) offers a means to quantify dispersion and polar interaction parameters in liquids, directly linking them to the intermolecular interactions [25]. This method has been applied to aqueous solutions containing salts [25] and ILs [26] using contact angle (CA) measurements with one polar and one non-polar reference liquid. Compared to other techniques, such as the acid-based theory (Oss and Good method [27–29]), the Zisman plot [30], and the Equation of State approach (Neumann method [31,32]), the OWRK method has proven more reliable. However, it has never been used to assess the dispersive and polar contributions of monophasic and biphasic regions of ATPS phase diagrams. It should be noted that, when applying the OWRK method to multicomponent mixtures, interfacial excesses and preferential adsorption of components at solid surfaces may lead to surface compositions that differ from those of the bulk [33,34]. As a result, the polar and dispersive contributions from contact angle measurements reflect not only bulk-phase characteristics but also surface adsorption effects. While this limits the direct interpretation of absolute values, the use of solid substrates with contrasting surface energy profiles helps to reduce the impact of such artifacts. Consequently, the OWRK method remains a valuable tool for comparative analysis, enabling tracking of polarity changes across mixture compositions and supporting correlations with macroscopic phenomena such as phase separation in ATPS.

In this study, we apply the OWRK method to determine the surface free energy components of binary and ternary mixtures of PEG600, PPG400, and H_2O across both monophasic and biphasic regions of the ternary system. The PEG600/PPG400/H_2O ATPS was selected as a proof-of-concept, as it is representative of polymer/polymer ATPS, systems known for their ultralow interfacial tensions and minimal polarity differences between coexisting phases. In previous work of our research group [6], we used computational tools to investigate the intermolecular interactions responsible for phase formation in ATPS composed of these two polyethers. These findings provide valuable support for the current study, which pioneers the use of OWRK method to assess the relative polarity of ATPS phases. The unique characteristics of polymer/polymer ATPS, and the PEG600/PPG400/H_2O system, in particular, make it an ideal model for demonstrating the sensitivity and reliability of the OWRK method.

This experimental approach captures the polarity variations within the immiscibility region by quantifying changes in the dispersive and polar forces of each phase. Initially, contact angles measurements on various polymeric materials surfaces using two reference liquids with known surface energy components, deionized water (H_2O) and dimethyl sulfoxide (DMSO). Based on these results, three materials (glass, polytetrafluoroethylene (PTFE) and polyethylene (PE)) were selected for further measurements using different various PEG600/PPG400/H_2O mixtures, in both monophasic and biphasic regions. The surface free energy of each mixture was then calculated and analysed in relation to composition and phase behaviour. This comprehensive study demonstrates that the OWRK method can serve as a simple and straightforward approach for quantifying the surface energy components of ATPS phases, yielding critical insights into the role of polarity differences in phase behaviour and solute partitioning mechanisms. These findings support the future development of tailored extraction systems optimized for efficiency and selectivity in solute recovery.

2. Experimental section

2.1. Materials

Polyethylene glycol with a molecular weight of 600 g/mol (PEG600) and polypropylene glycol with a molecular weight of 400 g/mol (PPG400) were both purchased from Sigma-Aldrich (USA).·H_2O used in this study underwent a double-distillation process, was passed through a reverse osmosis system, and subsequently purified with a Milli-Q plus 185 water purification system (H_2O resistivity of 18.2 MΩ·cm at 25 °C).

The solid substrates (polymeric materials) used for contact angles (CA) measurements included Ertalon®6 PLA (unmodified cast nylon 6 grade, referred to hereafter as PA), PE-HD/E (extruded high density polyethylene with a molecular weight of 500,000 g/mol, referred to as PE), Ertalyte® (polyethylene terephthalate, PET), polytetrafluoroethylene (PTFE), polyvinyl chloride (PVC), polyurethane (PU). These polymeric materials were kindly provided by PolyLanema, Lda. (Aveiro, Portugal). Glass microscopy slides used for CA measurements were obtained from Thermo Fischer Scientific (Madrid, Spain).

2.2. Phases composition and tie-line determination

Tie-lines (TLs) of biphasic systems were established by determining the weight percentages of PEG600 and PPG400 in each coexisting phase. H_2O content in each phase was quantified using Karl Fischer titration, performed with a Karl Fischer 890 Titrando instrument from Metrohm® (Switzerland), with an accuracy of ±0.5 %, at 25 ºC. HYDRANAL-methanol rapid (a reagent for accelerated volumetric one-component Karl Fischer titration) and HYDRANAL-Composite 5 (a methanol-free reagent for volumetric one-component Karl Fischer titration), both supplied by Sigma-Aldrich®, were used for the analysis. The polymer content in each phase was then calculated by subtracting the measured H_2O content (from Karl-Fischer titration) from the total mass, and subsequently intersecting the resulting polymer content values with the binodal curve to determine tie-lines. Further details of this graphical method for TLs determination are exemplified in Figure S1 (Supplementary Information, SI), with the composition of each phase, tie-line lengths (TLL) and TL slopes being presented in Table S1 (SI). All experiments were conducted in triplicate.

2.3. Contact angle measurements

Contact Angle (CA) measurements were performed using a Dataphysics Instruments GmbH (model OCA20, Germany). Droplets of 10 μL of each liquid sample were deposited onto the solid substrates at 25 ± 1 ºC. For each sample, whether for determining the surface energy of solid surfaces or evaluating the test mixtures, a minimum of five measurements was recorded. Before and after each set of measurements, all solid substrates were thoroughly cleaned using tissue paper moistened with 70 wt% aqueous ethanol solution, followed by rinsing with ultrapure H_2O. Any remaining was gently removed using laboratory-grade, lint-free tissue under clean bench conditions. This procedure ensured the removal of any surface contaminants that could interfere with accurate contact angle determination.

To calculate the surface energy of the solid substrates, literature-reported values for the surface energy components of H_2O and DMSO were used (Table 1) [35]. These two liquids were selected as reference standards, based on their prior validation for use the OWRK method [25,35].

The values presented in Table 1 were combined with the measured CA on each uncharacterized solid substrate, and used in the OWRK model to determine the polar and dispersive surface energy components of the substrates.

The characterized solid substrates with more distinct polar and dispersive contributions (*i.e.*, (glass, polytetrafluoroethylene (PTFE) and polyethylene (PE)) were then used to determine the surface energy components of unknown liquid mixtures. This was achieved by measuring the CA of the test mixtures on at least two different solid substrates and applying the OWRK model to obtain surface energy parameters.

The tested mixture compositions, both within the monophasic and biphasic regions of PEG600/PPG400/H_2O system, were selected based on the previously established ternary phase diagram at 25 ºC [6]. In addition, surface energy contributions of both polymer/H_2O mixtures with varying H_2O contents were also determined to support the interpretation of results for the ternary mixtures.

2.4. Owens-Wendt method

The surface energy of a solid material is typically determined through various methods, all derived from Young's equation, which minimizes the total interfacial interactions among solid (S), liquid (L), and gas (G) interfaces (Eq.1) [25,36]:

$$\gamma_{SG} = \gamma_{SL} + \gamma_{LG}\cos(\theta) \tag{1}$$

With γ_{SG}, γ_{SL}, and γ_{LG} representing the interfacial tensions at the solid-gas (SG), solid-liquid (SL), and liquid-gas (LG) interfaces, respectively, while θ is the contact angle measured between the liquid and the solid substrate.

However, Young's equation does not account for the specific SL interactions, or the molecular-level chemical forces involved in macroscopic CA measurements [25,36]. To address these limitations, several alternative models have been developed that build upon Young's foundational formula, aiming to provide a more comprehensive understanding of interfacial interactions.

One of the most widely used approaches is the OWRK model, an extension of Fowke's model. This model offers deeper insight into the SL and LG interactions that contribute for the observed contact angles [25,37].

While rooted 'in Young's equation, the OWRK model refines it by separating surface energy into two distinct interactions: dispersive (non-polar) and polar contributions (*e.g.*, $\gamma_S = \gamma_S^d + \gamma_S^p$). This separation enables a more accurate evaluation of surface energetics and interfacial

Table 1
Surface energy contributions of reference liquids H_2O and DMSO [35].

Reference Liquid	Surface energy contributions (mJ/m^2)		
	γ_L^d	γ_L^p	γ_L
H_2O	21.8	51	72.8
DMSO	36	8	44

phenomena, especially in complex liquid systems, allowing the derivation of the geometric-mean relationship for solid-liquid interfacial tension (γ_{SL}), as shown in Eq.2 [25,35]:

$$\gamma_{SL} = \gamma_S + \gamma_L - 2\sqrt{\gamma_S^d \gamma_L^d} - 2\sqrt{\gamma_S^p \gamma_L^p} \tag{2}$$

The final equation of the OWRK model is obtained by substituting Eq. 2 into Young's Eq. 1, and dividing both hand-sides by $\sqrt{\gamma_L^p}$ to yield the linearized form of Owens-Wendt model (Eq. 3), as previously reported [25,35]:

$$\frac{\gamma_L(1+\cos\theta)}{2\sqrt{\gamma_L^p}} = \sqrt{\frac{\gamma_L^d}{\gamma_L^p}}\sqrt{\gamma_S^d} + \sqrt{\gamma_S^p} \tag{3}$$

Using Eq. 3, the surface energy contributions of a solid substrate, specifically the γ_S^d and γ_S^p, can be determined by measuring the CA of at least two probe liquids with known polar components. In this study, the choice of H_2O and DMSO as reference liquids due to the inherently polar nature of ATPS phases, which are both H_2O-rich and thus exhibit substantial polar contributions to surface energy. This stands in contrast to conventional organic/aqueous liquid-liquid systems, where the polarity difference between phases is often more pronounced, and in some cases, one of the phases may consist primarily of a dispersive (non-polar) liquid.

It is important to note that the linearized form of the Owens–Wendt model (Eq. 3) is valid only when both reference liquids contain polar components. If at least one reference liquid lacks a polar contribution to its surface energy, a different linearization must be applied, specifically, by dividing both sides of Eq. 2 by $\sqrt{\gamma_L^d}$.

Since the total surface tension of a liquid is the sum of its dispersive and polar components (*i.e.*, $\gamma_L = \gamma_L^d + \gamma_L^p$), the corresponding dispersive and polar contributions of an unknown liquid can then be determined using Eq. 4 [25,35]:

$$\frac{\sqrt{\gamma_L^d}}{\gamma_L^d + \gamma_L^p}\sqrt{\gamma_S^d} + \frac{\sqrt{\gamma_L^p}}{\gamma_L^d + \gamma_L^p}\sqrt{\gamma_S^p} = 0.5(1+\cos\theta) \tag{4}$$

The unknown γ_L^p and γ_L^d components can be determined by measuring its CA on at least two solid substrates with well-characterized surface energy components [36,37]. By solving the resulting system of two equations with two unknown variables (*i.e.*, γ_L^p and γ_L^d), the surface energy components of the liquid can be accurately determined, as previously demonstrated for the determination of the liquid's surface energy components.

3. Results and discussion

Understanding polarity changes within an ATPS is crucial for elucidating the mechanisms that drive phase separation and solute partitioning, as polarity is closely associated with the intermolecular forces and thermodynamic behaviour of the system [16,18,38]. Building on our previous findings [6] and the theoretical framework outlined earlier, the novel application of OWRK model proposed in this study was carried out following the general procedure illustrated in Fig. 1.

Following the procedure presented in Fig. 1, the first step involved determining the surface energy contributions of seven solid substrates – PA, PE, PTFE, PET, PVC, and PU – using CA measurements with H_2O and DMSO, in accordance with the OWRK model. Based on these results, the three solid substrates with the most distinct polar and dispersive surface energy components were selected to evaluate the surface energy components of unknown liquids, including the coexisting phases of the PEG600/PPG400 ATPS and aqueous solutions of PEG600 and PPG400. The OWRK model was then applied to quantify polarity changes by analysing the surface energy contributions of both binary polymer/H_2O mixtures and ternary PEG600/PPG400/H_2O mixtures, across monophasic and biphasic regions. These results were then correlated with mixture compositions to provide molecular-level insights into the

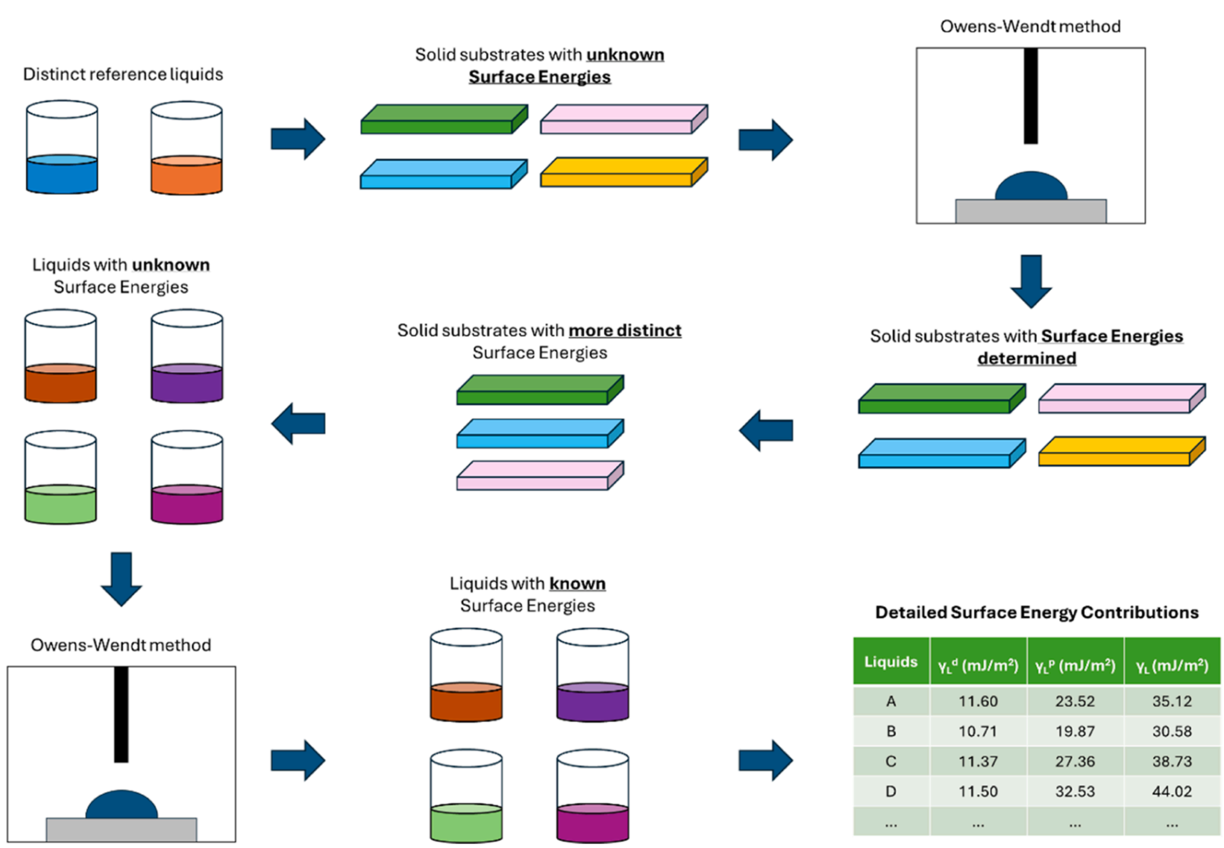

Fig. 1. Schematic representation of the general procedure used in this study, based on the Owens-Wendt-Rabel-Kaelble (OWRK) model.

dispersive and polar interactions that govern phase separation in polymer/polymer ATPS.

3.1. Surface energy components of solid substrates

The surface energy values of seven solid substrates were initially determined using two reference liquids. To begin, the surface energy components, specifically the dispersive (γ_S^d) and polar (γ_S^p) contributions, of each solid substrate were determined by measuring the CA of H_2O and DMSO on their surfaces. The measured CA values were then applied to Eq. 3, together with the known surface energy values of the two reference liquids (as listed in Table 1), using the OWRK model. The resulting CA data of both probe liquids on the solid substrates, along with the OWRK plots used for surface energy determination, are presented in Fig. 2.

As shown in Fig. 2A, DMSO resulted in lower CAs (*i.e.*, values between 31.90 ± 2.53 ° and 73.17 ± 2.93°) compared to H_2O (*i.e.*, values from 46.87 ± 5.03 ° to 106.41 ± 2.92 °) on all tested solid substrates. In general, higher CAs indicate weaker liquid-solid interactions, reflecting a greater mismatch between the surface energy components of the liquid and the solid [39,40]. Solid polymeric materials typically exhibit higher CAs with H_2O, as polymers tend to have a dominant dispersive surface energy contribution, while H_2O primarily exhibits polar surface energy characteristics [41,42]. Consequently, since DMSO has a higher dispersive contribution than H_2O (*i.e.*, γ_L^d values of 21.8 mJ/m^2 and 36 mJ/m^2 for H_2O and DMSO, respectively; see Table 1), it has stronger interactions with the polymeric solid substrates, resulting in lower contact angles.

Additionally, glass exhibited significantly lower contact angles, particularly for H_2O, compared to the polymeric material surfaces. This results from glass's inherently high surface energy, which is predominantly polar due to the abundance of hydroxyl groups (–OH) on its surface [43]. These hydroxyl groups facilitate strong interactions with highly polar protic solvents (*i.e.*, solvents containing an acidic hydrogen capable of forming structured hydrogen bonds, such as H_2O) and

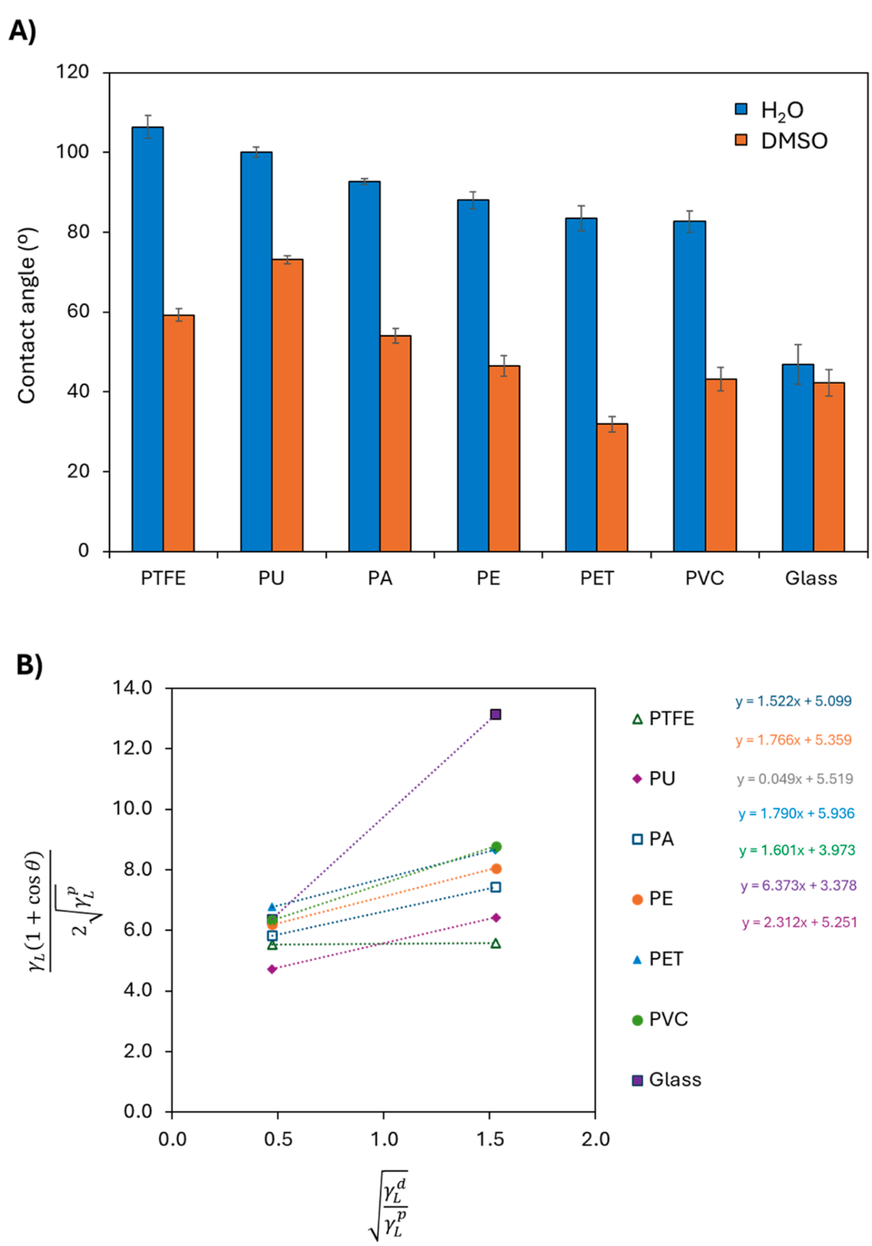

Fig. 2. Contact angle (CA) measurements (A) and Owens-Wendt (OWRK) plot (B) for all solid substrates tested using contact angles of H_2O and DMSO at 25 °C. The CA measurements are presented as the mean ± standard deviation, based on at least five independent measurements.

moderately polar aprotic solvents (*i.e.*, solvents that cannot donate hydrogen atoms but can act as hydrogen bond acceptors, such as DMSO). These interactions, primarily through hydrogen bonding and dipole-dipole forces, result in lower contact angles, typically ranging between 42 ° and 47 °. In contrast, polymeric materials, with their overall surface energy and limited polar functionality, exhibit weaker interactions with polar liquids, resulting in higher contact angles, particularly evident with H_2O [41,42]. As demonstrated by the contact angle measurements for H_2O in Fig. 2A, the polarity of each material follows the trend: PTFE < PU < PA < PE < PET < PVC < Glass, with PTFE being the most apolar surface and glass the most polar one.

Using the linearized OWRK plot shown in Fig. 2B, the polar and dispersive surface energy components of the seven solid substrates were calculated. In these plots, the slope of the linear regressions corresponds to the square root of dispersive component (γ_S^d), while the intercept corresponds to the square root of the polar component (γ_S^p). The calculated surface energy contributions are detailed in Table 2.

Table 2 shows that the glass slide exhibits the highest surface energy among the solid materials surfaces tested, with a strong polar contribution (*i.e.*, $\gamma_S = 52.03$ mJ/m^2, of which 40.62 mJ/m^2 arises from polar interactions). This distinct surface energy profile is attributed to the abundance of hydroxyl groups on the glass surface, which promote strong hydrogen bonding and dipole-dipole interactions with both reference liquids (H_2O and DMSO) [43].

In contrast, the polymeric materials displayed higher dispersive contributions (ranging from 18.35 to 38.44 mJ/m²) but lower total surface energies (maximum γ_S of 38.44 mJ/m^2 for PE and PET) in comparison to glass ($\gamma_S^d = 11.41$ mJ/m^2, with a γ_S of 52.03 mJ/m^2). These values are consistent with the inherently lower surface energy typically observed in polymers, as previously reported [42]. The most notable difference between the polymeric materials lies in their polar contributions, which range from 0.00 to 5.34 mJ/m^2 and closely correlate with their respective H_2O contact angles (PTFE < PA < PU < PE < PET < PVC < Glass). This trend indicates that the contact angle with H_2O is a reliable measure of the polar contribution of the polymeric surfaces.

Given that these solid substrates were to be used for determining the surface energy of aqueous solutions, and that greater contrast in surface energy components improves the accuracy of OWRK calculations [25], three substrates with the most distinct surface energy profiles – glass, PE, and PTFE – were selected for further analysis. Moreover, the distinct surface energy contributions of these materials enhance their representativeness with respect to ATPS, as they span a broad range of polar and dispersive interactions. This diversity enables a more accurate and comprehensive evaluation of the surface energy characteristics of the studied mixtures. The polarity of each aqueous mixture was then determined by measuring the CA on these substrates and calculating the liquid's surface energy using the OWRK model applied to the glass/PE and glass/PTFE combinations. For each aqueous mixture, average surface energy values and their corresponding dispersive and polar components were derived from the results with the two substrate pairs.

The following sections present the results for binary and ternary mixtures, relating the behaviour of monophasic and biphasic aqueous systems to phase polarity using the OWRK method, and offering deeper insight into phase separation and solute partitioning mechanisms.

Table 2
Surface energy contributions of all solid substrates (i.e., Ertalon®6 PLA (unmodified cast nylon 6 grade, PA), PE-HD/E (extruded high density polyethylene with a molecular weight of 500,000 g/mol, PE), Ertalyte® (polyethylene terephthalate, PET), polytetrafluoroethylene (PTFE), polyvinyl chloride (PVC), polyurethane (PU), and glass), calculated using the Owens-Wendt (OWRK) model based on contact angle measurements with H_2O and DMSO at 25 ºC.

Substrates	γ_S^d (mJ/m^2)	γ_S^p (mJ/m^2)	γ_S (mJ/m^2)
PTFE	30.45	0.00	30.46
PU	15.79	2.56	18.35
PA	26.00	2.32	28.31
PE	28.73	3.12	38.44
PET	35.24	3.20	38.44
PVC	27.57	5.34	32.92
Glass	11.41	40.62	52.03

3.2. Polarity of polymer/H_2O binary mixtures

Before evaluating the polarities of ternary mixtures and ATPS coexisting phases, it is essential to first understand how the surface energy changes in binary aqueous mixtures containing the individual polymers. To this end, contact angles were measured and the corresponding surface energy components were calculated for PEG600/H_2O and PPG400/H_2O mixtures across varying H_2O contents. This analysis provides insights into how the intermolecular interactions between each polymer and H_2O evolve with composition, which is critical for understanding the behavior of the PEG600/PPG400-based ATPS.

Contact angle measurements were performed on three solid substrates: glass, PTFE, and PE. The surface energy values, along with their polar and dispersive components, were calculated by averaging the results obtained from applying the OWRK model to the glass/PTFE and glass/PE pairs. These values are presented in Fig. 3 for both the PEG600/H_2O and PPG400/H_2O systems. These results serve as reference points for interpreting the polarity shifts observed later in the ternary mixtures and the ATPS coexisting phases.

The results presented in Fig. 3 show that PEG/H_2O mixtures exhibited higher CA values than PPG400/H_2O on PE and PTFE (*i.e.*, CAs between 60 ° and 100 ° for PEG600/H_2O and from 40 ° to 70 ° for PPG400/H_2O). On glass, however, the CA values fall within a similar range, approximately 20 ° to 50 °. These differences can be attributed to the distinct molecular structures and surface energy characteristics of PEG600 and PPG400.

PPG400 has a more apolar structure than PEG600 due to the presence of additional methyl groups (-CH_3) in its polymer backbone. These groups reduce H_2O affinity and solubility [6,44], leading to weaker PPG400-H_2O interactions and stronger dispersive interactions with more apolar surfaces, such as PE and PTFE. This promotes greater spreading of the PPG400/H_2O mixtures on these solid substrates, resulting in lower CA values [42,45].

In contrast, PEG600, lack these more hydrophobic methyl groups and exhibits greater polarity, primarily due to its terminal hydroxyl (–OH) groups, which form strong hydrogen bonds with H_2O. This interpretation is supported by our previous findings [6], which showed that PEG600 interacts approximately 30 % more favourably with H_2O than PPG400 in terms of OH–OW interactions, and up to 100 % more favourably for OE–OW interactions as H_2O content increases. The hydrophobic methyl groups in the PPG400 chain hinder hydrogen bond formation, decreasing its affinity for H_2O compared to PEG600 [6]. As a result, aqueous mixtures containing PEG600 are more polar than those with PPG400. Consequently, they interact less favourably with apolar surfaces, leading to higher CA values on PE and PTFE [43,45].

Distinct trends were also observed as polymer content increased. On the glass substrate, the CA values increased for both PEG600/H_2O and PPG400/H_2O mixtures, reflecting a decrease in overall mixture polarity as H_2O content diminished due to the reduced number of H_2O molecules interacting with the highly polar glass surface.

For PE and PTFE, the trends of the two polymer aqueous mixtures diverged. PEG600/H_2O mixtures showed decreasing CA values with increasing polymer content, indicating that the mixture become more compatible with the apolar surfaces due to enhanced dispersive interactions and decreased polarity. On the other hand, CAs increased with polymer content in PPG400/H_2O mixtures for PE and was almost constant for PTFE. As the latter one presents only dispersive contributions in its total surface energy, the similar CA values across all polymer concentrations (between 62.50 ± 3.15 ° and 68.23 ± 5.36 °) indicate that the dispersive forces of the mixtures do not change significantly

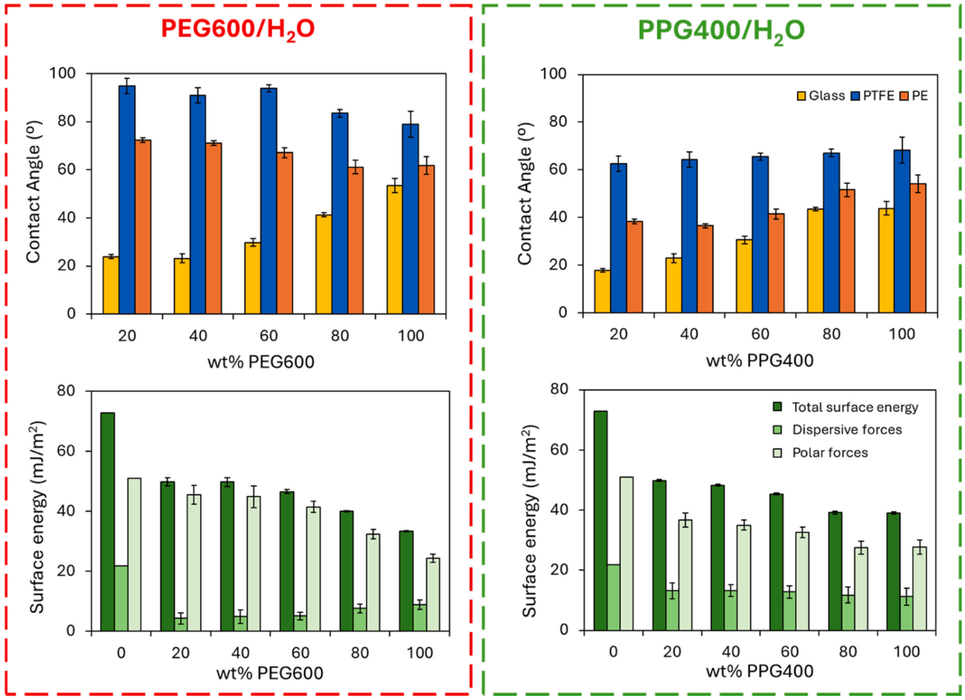

Fig. 3. Contact angles and surface energies (total, dispersive and polar) of PEG600/H_2O and PPG400/H_2O mixtures at varying H_2O contents. Data are shown for measurements conducted on glass, PTFE, and PE substrates. The columns corresponding to 0 wt% polymer represent the surface energy components of pure H_2O, as reported in literature [35] and listed in Table 1.

with composition. This behaviour is attributed to PPG400's lower polarity, *i.e.*, weaker hydrogen bonding with H_2O, and its tendency to self-associate in aqueous media [6,23]. As polymer content increases, self-aggregation becomes more prominent, reducing the availability of polymer chains to interact with the solid apolar surfaces and thereby limiting wetting (*i.e.*, resulting in higher CA values). Unlike PTFE, PE has a polar contribution to its total surface energy (Table 2). As the dispersive contribution appears constant (as indicated by the behaviour on PTFE), the higher CA values observed for PE at higher polymer concentrations (increasing from 38.35 ± 1.07 ° to 54.09 ± 3.71 °) are attributed to the decreasing number of H_2O molecules in the mixtures with increasing polymer concentration. This decrease lowers the polarity of the binary mixtures, leading to less polar interactions with the PE surface and, consequently, higher CA values.

These interpretations are supported by the corresponding surface energy data. As polymer content increases, the polarity of both types of mixtures decreases due to the lower number of H_2O molecules and resulting reduction of hydrogen bonding. However, the dispersive forces behave differently. For PEG600/H_2O mixtures, dispersive contributions increase gradually with polymer concentration, indicating a shift from hydrogen-bonding (polar)-dominated interactions to dispersion-dominated. In contrast, PPG400/H_2O mixtures maintain relatively constant dispersive contributions across all compositions. This is consistent with PPG400's lower polarity and its self-association behaviour [6,23], which reduces the number of available nonpolar groups for surface interaction with apolar surfaces, and explains the almost constant CA values for all substrates when the test mixtures contain 80 % and 100 % of PPG400.

Overall, these findings emphasize the distinct intermolecular interactions governing the wetting behaviour of PEG600 and PPG400 mixtures. The OWRK model effectively captures these differences, corroborating earlier observations that hydrogen-bonding in PEG600 and self-aggregation PPG400 are key drivers of phase separation in PEG600/PPG400 ATPS [6].

Building on these insights, the next section explores the surface energy characteristics of monophasic and biphasic ternary mixtures composed of PEG600, PPG400, and H_2O, and correlates them with the ATPS phases' composition and overall system polarity.

3.3. Polarity of PEG600/PPG400/H_2O mixtures

The mixture points investigated in this study were selected based on the phase diagram profile and the analysis reported in a previous work, specifically mixture points B3, M4, and M5 [6]. To further investigate polarity variations across different regions of the ternary phase diagram, three additional monophasic (M) mixtures (M1, M2, and M3), corresponding to H_2O-rich regions, and three additional mixtures (B1, B2, and B4) within the biphasic region were prepared and analysed. These nine mixture points were chosen to provide a comprehensive overview of the ternary phase diagram, covering a wide range of compositions and phase behaviours, including transitions from monophasic to biphasic states. This approach not only allows a better understanding of how phase equilibrium properties vary across different regions but also enables a more thorough assessment of surface energy components and polarity contrasts throughout the ternary system.

For biphasic mixtures, the surface energy components of each coexisting phase were independently determined and correlated with their compositions, which were obtained *via* tie-line (TL) analysis. This approach allowed for a direct evaluation of how compositional differences affect phase polarity in PEG600/PPG400/H_2O system. The complete ternary phase diagram, along the location of all evaluated mixture points, is shown in Fig. 4.

Based on the mixture points shown in Fig. 4, contact angles for all monophasic and biphasic mixtures were measured (*cf.* Figure S2 in SI), and their corresponding surface energy components were calculated using the OWRK model. The resulting polar and dispersive contributions for each mixture, and for each individual phase in the biphasic systems, are presented in Fig. 5.

One of the most striking features of Fig. 5 is that all ternary mixtures exhibit significantly lower surface energy values than pure H_2O. This reduction is due to the presence of PEG600 and PPG400, both of which possess substantially lower surface free energies (35–40 mJ/m^2) than

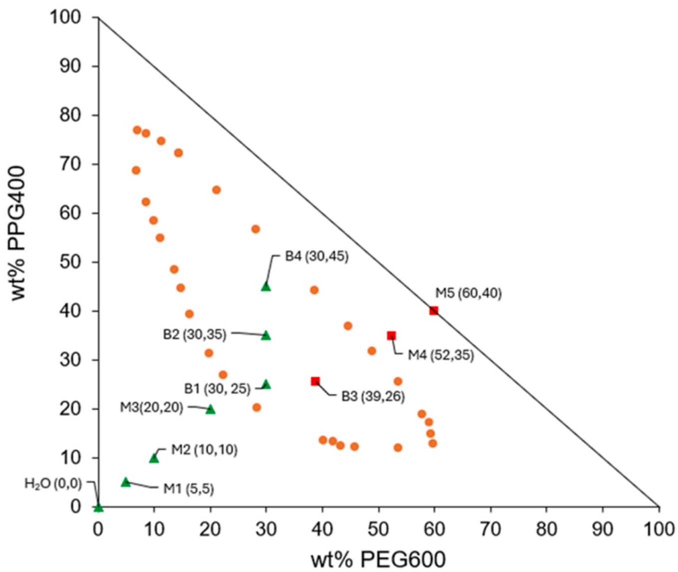

Fig. 4. Ternary phase diagram of PEG600/PPG400/H_2O ATPS at 25 °C. Mixtures points marked with red squares (■) corresponded to those previously reported by Jorge *et al.* [6], while the new mixture points investigated in this study are indicated by green triangles (▲). The composition of each mixture is defined by its PEG600 and PPG400 weight fraction (%) coordinates. The origin of the plot (0,0), point labelled H_2O, corresponds to pure H_2O (100 wt%). Mixture points labelled "M" and "B" correspond to monophasic and biphasic systems, respectively, and are ordered by decreasing H_2O content. For biphasic systems, the compositions of the top and bottom phases, along with their respective tie-line lengths (TLL) and slopes, are provided in Table S1.

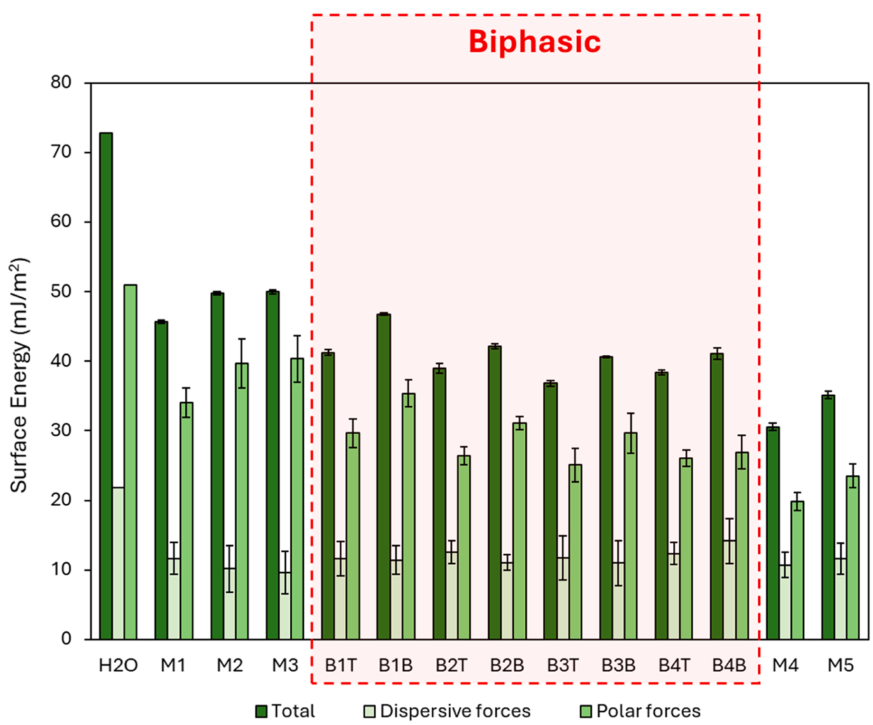

Fig. 5. Surface energy components (dispersive and polar) of the monophasic and biphasic PEG600/PPG400/H_2O mixtures. Labels "T" and "B" refer to the top and bottom phases of each biphasic mixture, respectively (*e.g.*, B1T and B1B correspond to the top (PPG400-rich) and bottom (PEG600-rich) phases of mixture B1). The red dotted square highlights the biphasic mixtures to facilitate comparison with the monophasic systems. The H_2O point represents pure H_2O (100 wt%), with its polar and dispersive components sourced from literature [35].

H_2O (~72 mJ/m^2) [35]. The incorporation of these polymers weakens the cohesive intermolecular forces within the system, particularly hydrogen bonding among H_2O molecules, thereby reducing the overall surface energy of the polymeric aqueous solutions [41,42].

From pure H_2O to M1, a decrease in the surface energy and polar forces is observed. However, as the polymer content increases from M1 to M2 and M3, the system displays a clear increase in polar contributions constant, ranging from 34.03 ± 2.11–40.39 ± 3.35 mJ/m^2, while the dispersive components remain relatively constant (*i.e.*, between 11.60 ± 2.31 and 9.60 ± 3.04 mJ/m^2). This behaviour is related to the differences in the interaction of PEG600 and PPG400 with H_2O at increasing polymer concentrations. As shown in Fig. 3, PPG400 interacts weakly with H_2O, resulting in minimal changes in the dispersive contribution, even at higher polymer concentration [8,23,46].

Consequently, increasing the amount of PPG400 in the ternary system has little impact on the overall surface energy profile. In contrast, PEG600, is more hydrophilic and forms an increasing number of hydrogen bonds with H_2O as its concentration increases, thereby enhancing the polarity characters of the ternary mixtures.

The combination of PPG400's weak affinity for H_2O and PEG600's strong hydrogen bonding interactions at higher polymer concentrations results in a progressively more polar system. This trend correlates with the onset phase separation observed at B1. As the polymer content continues to increase, the polarity difference between PEG600–H_2O clusters and PPG400 becomes increasingly pronounced. Once this polarity exceeds a critical threshold, macroscopic phase separation occurs.

These observations are consistent with previous reports and are associated with the more hydrophilic nature of PEG600 and the hydrophobic character of PPG400. They also reinforce the observations from Fig. 3, indicating that system polarity is predominantly driven by PEG600–H_2O interactions, whereas the self-association of PPG400 contributes to constant dispersive profile across compositions [8,23].

Upon transitioning from a monophasic to a biphasic regime (*i.e.*, from M3 to B1–B4), Fig. 5 reveals a notable decline in both total surface energy (from 49.99 mJ/m^2 in M3, to 41.27 mJ/m^2 in B1T and 46.78 mJ/m^2 in B1B) and polar contributions (from 40.39 mJ/m^2 in M3, to 29.68 mJ/m^2 in B1T and 35.37 mJ/m^2 in B1B) in each coexisting phase compared to the monophasic mixtures. This decline reflects the separation of PPG400 and PEG600 into distinct top and bottom phases, respectively, leading to a reduction in overall polarity [41,42]. Although PEG600 concentration increases in the bottom phase from B1 to B4, the total H_2O content decreases (*cf.* Table S1), thereby reducing polarity and total surface energy.

In all biphasic systems, the PEG600-rich (bottom) phases consistently exhibit higher polarity than the PPG400-rich (top) phases. This disparity highlights the greater ability of PEG600 to form hydrogen bonds with H_2O, while PPG400, being more hydrophobic and sterically hindered, interacts weakly with H_2O and maintains a lower polarity and a relatively stable dispersive contribution [6,8,24].

As briefly introduced above, the observed polarity decrease in both phases of the biphasic ternary mixtures aligns with the behaviour of their corresponding PEG600-H_2O and PPG400-H_2O mixtures (*cf.* Fig. 3). As total polymer content increases, the H_2O content in the system decreases, limiting hydrogen bonding and leading to a lower polarity. This reduction is more pronounced in the PEG-rich (bottom) phases, where the polar contributions decrease from 35.37 ± 1.93 to 26.93 ± 2.39 mJ/m^2, compared to a smaller decrease in the PPG400-rich (top) phase (*i.e.*, from 29.68 ± 2.07 to 26.06 ± 1.21 mJ/m^2). A similar trend evident in the binary mixtures: polarity decreases from 45.49 ± 3.19 to 24.38 ± 1.42 mJ/m^2 for PEG600-H_2O and from 36.66 ± 2.38 to 27.81 ± 2.34 mJ/m^2 for the PPG400-H_2O binary mixtures, as polymer content increases from 20 % to 100 %. The more substantial drop in the polarity for PEG600-based systems is attributed to the decreasing number of H_2O molecules available to form hydrogen bonds, leaving a growing fraction PEG600 molecules non-hydrated. This results in reduced polarity and a shift in surface energy balance toward dispersive contributions.

A similar, though less pronounced, trend is observed for PPG400. Due to its inherently weaker interaction with H_2O, the decrease in polarity of the PPG400-rich (top) phases with increasing polymer concentration is more modest. Notably, in mixture B4, the polarities of the top and bottom phases become nearly identical. This convergence marks the transition from biphasic (B4) to monophasic (M4) region. As polymer concentration increases and H_2O content decreases, polarity contrast between phases diminishes. The reduced hydration of both polymers enhanced polymer-polymer interactions, ultimately resulting in fully miscible, monophasic regime at high polymer concentrations.

This transition from the biphasic to the monophasic region at lower H_2O content (*i.e.*, from B4 to M4 and M5) is accompanied by a further decrease in total surface energy values and ATPS polarity. At these high polymer concentrations, the system no longer behaves as typical aqueous solutions but rather as a hydrated polymer mixture, where polymer–H_2O interactions are minimal. The differential hydration of the two polymers, that previously drove phase separation is no longer possible, and the system is dominated by favourable interactions between the two polymers [6,8,9,24]. As a result, the system becomes more miscible, due to favourable PEG600–PPG400 interactions, favouring monophasic mixtures over biphasic separation. Our previous results showed that segregation between PPG400 and PEG600 required moderate H_2O contents, when PPG400 self-aggregates and excludes PEG600–H_2O clusters, leading to the phase separation [6].

Interestingly, while dispersive contributions remain stable across all compositions – hovering 10 mJ/m^2 – the most significant variation in surface energy arises from changes in polar contributions. This observation suggests that changes in the system polarity, rather than dispersion, plays the dominant role in governing phase separation.

To explore this further, we calculated the mean values of each surface energy component and determined three ratios to assess the balance between dispersive and polar forces:

- **D/T:** Dispersive-to-total surface energy ratio
- **P/T**: Polar-to-total surface energy ratio
- **D/P**: Dispersive-to-polar surface energy ratio.

The individual ratios for each monophasic mixture and for each phase of the biphasic systems are shown in Fig. 6.

Fig. 6 shows clear variations in the surface energy ratios (D/T, P/T, and D/P) across the investigated mixtures. Among these, the highest values are recorded for P/T ratio, ranging from 0.65 to 0.81, while the D/T ratio exhibits the lowest values (from 0.19 to 0.35). In the first monophasic region (from pure H_2O to M3), the P/T ratio increases from 0.70 to 0.81, indicating a growing dominance of polar interactions. Concurrently, D/P and D/T ratios decreased from 0.43 to 0.24 and from 0.30 to 0.19, respectively, reflecting the increasing influence of hydrogen bonding and PEG600-H_2O clusters polarity as the polymer concentration increases. Within the biphasic region (B1 – B4), a different trend emerges. For the PPG400-rich (top) phases (dotted bars in Fig. 6), P/T decreases slightly from 0.72 to 0.68, D/P increases from 0.39 to 0.48, and D/T increases from 0.28 to 0.32. Similarly, for the PEG600-rich (bottom) phases (dashed bars in Fig. 6), P/T decreases from 0.76 to 0.66, while D/P and D/T increase from 0.32 to 0.52 and from 0.24 to 0.34, respectively. These trends indicate a decrease in polarity across the phases, accompanied by relatively greater contributions from dispersive interactions as H_2O content decreases and polymer concentrations increases. In the second monophasic region (M4 and M5), a slight rebound in P/T is observed (from 0.65 to 0.67), alongside with a modest decrease in both D/P (from 0.54 to 0.49) and D/T (from 0.35 to 0.33). This shift reflects the system's transition into a highly concentrated polymer regime, where dispersive forces and polymer–polymer interactions dominate. The slight increase in polarity is attributed to residual H_2O molecules surrounding PEG600–PPG400 clusters, which continue to contribute weakly to hydrogen bonding, thereby maintaining a small but measurable polar component in the system.

Although dispersive contributions appeared relatively stable in Fig. 5, changes in the *ratios* are still noticeable. These variations primarily stem from differences in polar contributions, as the dispersive forces remain relatively constant across all mixtures. The increase in P/T ratio from M1 to M3 is attributed to enhanced hydrogen bonding between PEG600 and H_2O molecules, as more PEG600 is hydrated for increasing polymer content in the ternary mixture, while PPG400 weakly interacts with H_2O and does not significantly influence the system's surface energy [6,46]. This growing polarity correlates with the subsequent transition from a monophasic to a biphasic regime (M3 to B1), reflecting stronger PEG–H_2O interactions, and consequently segregation of PPG400 for an opposite immiscible phase. The formation of PEG600–H_2O clusters with higher polarity, driven by intensified hydrogen bonding, leads to phase separation when the polarity contrast

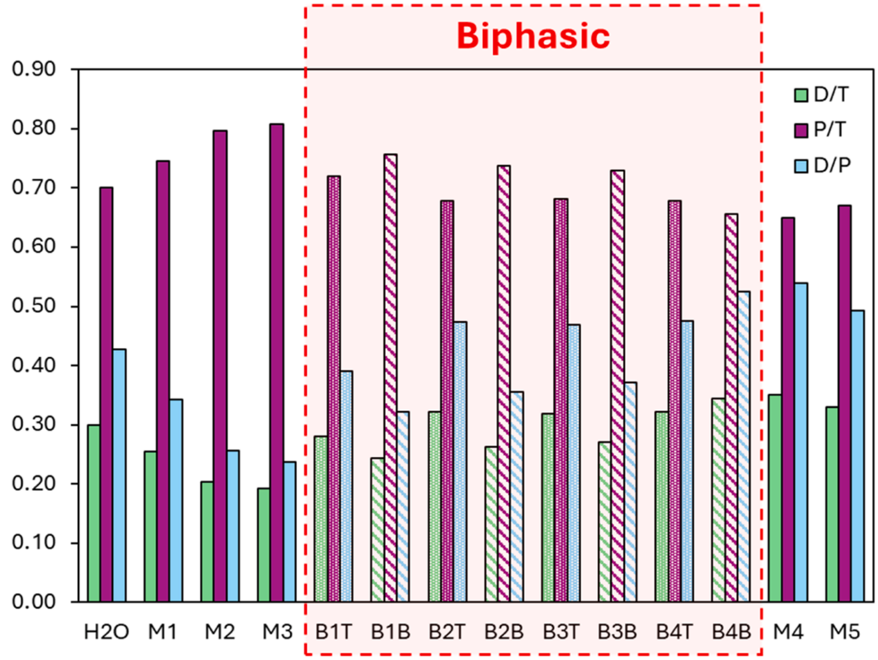

Fig. 6. Surface energy ratios for all investigated PEG600/PPG400/H_2O mixture points. The ratios include D/T (dispersive forces to total surface energy) (green bars), P/T (polar forces to total surface energy) (purple bars), and D/P (dispersive forces to polar forces) (blue bars). The red dotted square highlights the biphasic mixtures: dotted bars represent PPG400-rich (top) phases, and dashed bars represent PEG600-rich (bottom) phases. Solid-coloured bars correspond to monophasic systems, enabling direct comparison between monophasic and biphasic systems.

with PPG400 surpasses a critical threshold (P/T ratio $>$ 0.80, and D/T ratio $<$ 0.20). These results demonstrated that the stronger PEG600–H_2O interactions, combined with PPG400's hydrophobic nature and steric hindrance, promote macroscopic segregation once H_2O content reaches a certain level [6,9,23].

Within the biphasic region, once the critical polarity threshold is reached (*i.e.*, P/T $>$ 0.8), the polar ratio progressively decreases from B1 to B4, eventually reaching values comparable to those observed in monophasic mixtures (*i.e.*, P/T $\approx$ 0.7). At this point, the compositions of the ternary mixtures again become thermodynamically favourable for full miscibility, and the macroscopic biphasic system transitions back into a monophasic state.

In general, the P/T values of the PEG600-rich (bottom) phases are higher than those of the PPG400-rich (top) phases, while the D/T and D/P values follow the opposite trend This behaviour is consistent with the stronger hydrogen bonding between PEG600 and H_2O molecules, in contrast to the weaker interactions between PPG400 and H_2O. The progressive decrease in polarity difference between the two phases across the biphasic region (from B1 to B4) is attributed to declining H_2O content in the coexisting phases. As the H_2O content decreases, the system's capacity for hydrogen bonding is reduced, leading to an overall decrease in polarity. Simultaneously, the D/P and D/T ratios increase, reflecting a relatively stable contribution from dispersive forces alongside a marked reduction in polar interactions. This shift alters the balance of intermolecular interactions, steering the system toward a less polar system and minimizing polarity differences between the phases. This trend becomes particularly evident at the highest polymer concentration within the biphasic region (B4), where the polarity of the PEG-rich (bottom) phase approaches that of the PPG-rich (top) phase. This convergence suggests that the system is approaching a phase transition, with the potential to re-enter a monophasic regime as the total polymer concentration continues to increase in the ternary mixture.

As the system evolves from B4 (biphasic) to M4 and M5 (monophasic), the continued increase in polymer concentration and further depletion of H_2O content weaken the hydrogen bonding between PEG600 and H_2O molecules. This leads to a further reduction in the polarity contrast between PEG600-H_2O clusters and PPG400. When dispersive interactions become more significant and the polarity difference falls below the critical threshold required for phase segregation, the system transitions back to a fully miscible again, monophasic state.

These findings indicate that the phase demixing in the PEG600/PPG400 ATPS is fundamentally governed by the polarity difference between PEG600/H_2O clusters and the steric-driven self-association of PPG400. In H_2O-rich mixtures, PEG600 increases mixture polarity via extensive hydrogen bonding with H_2O, and phase separation is triggered when the resulting PEG600-H_2O clusters differ significantly in polarity from the more hydrophobic PPG400. However, as polymer concentration rises and H_2O content diminishes, hydrogen bonding becomes limited, polarity differences decrease, and favourable dispersive interactions between polymers emerge, ultimately restoring miscibility.

Overall, these results validate previous thermodynamic and computational studies [6] and provide new experimental insights into the polarity-driven mechanisms underlying PEG600/PPG400 ATPS formation. This study demonstrates the effectiveness of the Owens-Wendt method for quantifying the polarity changes of ATPS, particularly in polymer/polymer systems characterized by ultralow interfacial tensions and minimal polarity differences between coexisting phases [15,16,47]. The sensitivity of this method highlights its potential as a powerful tool for advancing research in complex liquid–liquid systems. By applying this approach, researchers can gain a deeper understanding of the intermolecular interactions that drive phase separation and solute partitioning in advanced LLE systems.

Despite the successful use of the OWRK model to assess the relative polarity of ATPS phases, we emphasize that the methods' accuracy and precision depend heavily on the choice of linearization approach, reference liquids, and solid substrates. For more conventional organic/aqueous liquid-liquid systems, it is advisable to use a broader range of reference liquids with distinct polar and dispersive properties, along with carefully selected solid substrates. Furthermore, reference liquids should be chemically and thermally stable under testing conditions and compatible with the solid surfaces used. The selection of solid substrates is also critical, as factors such as surface polarity, chemical compatibility with test liquids, and surface uniformity can influence wetting behaviour and introduce variability in contact angle measurements. Using substrates that span a wide polarity range and are chemically inert enhances the robustness of the analysis. Incorporating both hydrophilic and hydrophobic substrates provided a broader surface energy contrast, thereby enhancing the reliability of the OWRK model. Furthermore, as the model captures both bulk properties (arising from the mixture compositions) and interfacial phenomena (resulting from surface adsorption effects), the resulting values should be interpreted as comparative indicators, rather than absolute measures of polarity. When these considerations are carefully accounted for, this approach proves to be a powerful and informative tool for identifying polarity trends and correlating them to phase separation behaviour, an interpretation further supported by the strong agreement between our results and previous experimental observations as well as bulk-phase molecular simulations.

4. Conclusions

This study explored the potential of the Owens-Wendt method for analysing polarity changes that drive ATPS formation and partition mechanisms. Surface energy contributions of various substrates were first determined using H_2O and DMSO as reference liquids, with PTFE (γ_S^d = 30.45 mJ/m^2; γ_S^p = 0.00 mJ/m^2), PE (γ_S^d = 28.73 mJ/m^2; γ_S^p = 3.12 mJ/m^2), and glass (γ_S^d = 11.41 mJ/m^2; γ_S^p = 40.62 mJ/m^2) exhibiting the most distinct surface energy characteristics. The Owens-Wendt method was then applied to assess the surface energy contributions of binary polymer/H_2O and ternary PEG600/PPG400/H_2O mixtures using contact angle measurements and the PTFE/glass and PE/glass pairs. The addition of PEG600 and PPG400 reduced both polar and dispersive contributions in the binary systems, with dispersive forces increasing as PEG600 content rose (from 4.3 to 8.9 mJ/m^2, for polymer content increasing from 20 and 100 %wt, respectively), while remaining largely unchanged for varying PPG400 concentrations (from 13.2 to 11.2 mJ/m^2, for polymer content increasing from 20 and 100 %wt, respectively). The smaller dispersive contributions in PEG600 mixtures reflected their higher polarity due to stronger hydrogen bonding with H_2O, whereas PPG400's hydrophobic nature and weaker interactions with H_2O were evident in its stable dispersive forces across different polymer concentrations. These findings are consistent with prior observations from computational studies.

These findings were then linked to the surface energy contributions of ternary mixtures and the transition between monophasic and biphasic regimes. The formation and disruption of hydrogen bonds between PEG600/H_2O clusters were identified as key drivers of phase separation. In H_2O-rich systems, higher PEG600 concentrations led to stronger hydrogen bonding, increasing the polarity of PEG600/H_2O clusters and amplifying their polarity contrast with PPG400, thereby inducing phase separation. As polymer concentration increased and H_2O content decreased in biphasic mixtures, polarity differences between phases diminished, eventually leading to a monophasic regime driven by stronger apolar intermolecular interactions. Analysis of the Dispersive-to-Polar (D/P) force ratio revealed that phase separation occurred when $D/P < 0.24$, with the ratio increasing across biphasic region mixtures as polymer content rose. A transition to a new monophasic region was observed once the D/P ratio exceeded 0.50.

In conclusion, this study demonstrated that the Owens-Wendt method, when applied with a clear understanding of its limitations, provides a sensitive and reliable approach for assessing the relative polarity of ATPS. By correlating polarity variations with system phase separation mechanisms and solute distribution, the methodology contributes to a deeper understanding of ATPS behaviour and supports the design of optimized extraction processes for different target molecules.

CRediT authorship contribution statement

Alexandre M.S. Jorge: Conceptualization, Methodology, Software, Validation, Investigation, Formal analysis, Data Curation, Visualization, Writing - Original Draft, Writing - Review & Editing. **João A. P. Coutinho:** Conceptualization, Methodology, Validation, Resources, Writing - Review & Editing, Project Administration, Funding acquisition. **Jorge F. B. Pereira:** Conceptualization, Methodology, Validation, Resources, Data curation, Visualization, Supervision, Writing- Reviewing and Editing, Project Administration, Funding Acquisition.

Declaration of Generative AI and AI-assisted technologies in the writing process

During the preparation of this study, ChatGPT was used to improve the readability and language of the manuscript. After using this tool/service, the authors reviewed and edited the content as required and took full responsibility for the publication.

Declaration of Competing Interest

The authors declare that they have no known competing financial interests or personal relationships that could have appeared to influence the work reported in this paper.

Acknowledgements

This work was partly developed within the scope of the project CICECO-Aveiro Institute of Materials, UIDB/50011/2020, UIDP/50011/2020 & LA/P/0006/2020, financed by national funds through the FCT/MCTES (PIDDAC). CERES is supported by the Fundação para a Ciência e a Tecnologia (FCT) through the projects UIDB/EQU/00102/2020 and UIDP/EQU/00102/2020. J.F.B. Pereira and A. M. S. Jorge acknowledge FCT for funding the project DRI/India/0044/2020 and Fundação Calouste Gulbenkian for funding the project DYELOOP.

Appendix A. Supporting information

Supplementary data associated with this article can be found in the online version at doi:10.1016/j.colsurfa.2025.138080.

Data Availability

Data will be made available on request.

References

[1] A.M.S. Jorge, J.F.B. Pereira, Aqueous two-phase systems – versatile and advanced (bio)process engineering tools, Chem. Commun. 60 (2024) 12144–12168, https://doi.org/10.1039/D4CC02663B.
[2] M. Iqbal, Y. Tao, S. Xie, Y. Zhu, D. Chen, X. Wang, L. Huang, D. Peng, A. Sattar, M.A.B. Shabbir, H.I. Hussain, S. Ahmed, Z. Yuan, Aqueous two-phase system (ATPS): an overview and advances in its applications, Biol. Proced. Online 18 (2016) 18, https://doi.org/10.1186/s12575-016-0048-8.
[3] P.-Å. Albertsson, Partition of proteins in liquid polymer–polymer two-phase systems, Nature 182 (1958) 709–711, https://doi.org/10.1038/182709a0.
[4] J. Sinha, P.K. Dey, T. Panda, Aqueous two-phase: the system of choice for extractive fermentation, Appl. Microbiol Biotechnol. 54 (2000) 476–486, https://doi.org/10.1007/s002530000342.
[5] J.C. Merchuk, B.A. Andrews, J.A. Asenjo, Aqueous two-phase systems for protein separation, J. Chromatogr. B Biomed. Sci. Appl. 711 (1998) 285–293, https://doi.org/10.1016/S0378-4347(97)00594-X.
[6] A.M.S. Jorge, G.M.C. Silva, J.A.P. Coutinho, J.F.B. Pereira, Unravelling the molecular interactions behind the formation of PEG/PPG aqueous two-phase systems, Phys. Chem. Chem. Phys. 26 (2024) 7308–7317, https://doi.org/10.1039/D3CP05539F.
[7] A.R. Titus, P.P. Madeira, L.A. Ferreira, V.Y. Chernyak, V.N. Uversky, B.Y. Zaslavsky, Mechanism of phase separation in aqueous two-phase systems, Int J. Mol. Sci. 23 (2022) 14366, https://doi.org/10.3390/ijms232214366.
[8] M. Malmsten, P. Linse, K.W. Zhang, Phase behavior of aqueous poly(ethylene oxide)/poly(propylene oxide) solutions, Macromolecules 26 (1993) 2905–2910, https://doi.org/10.1021/ma00063a040.

[9] Å. Gustafsson, H. Wennerström, F. Tjerneld, The nature of phase separation in aqueous two-polymer systems, Polymer 27 (1986) 1768–1770, https://doi.org/10.1016/0032-3861(86)90274-0.
[10] A.M.S. Jorge, J.A.P. Coutinho, J.F.B. Pereira, Hydrodynamics of cholinium chloride-based aqueous biphasic systems (ABS): a key study for their industrial implementation, Sep Purif. Technol. 320 (2023) 124183, https://doi.org/10.1016/j.seppur.2023.124183.
[11] J.F.B. Pereira, J.A.P. Coutinho, Chapter 5 - aqueous Two-Phase systems, in, in: C. Poole (Ed.), Liquid-Phase Extraction, Elsevier, 2020, pp. 157–182, https://doi.org/10.1016/B978-0-12-816911-7.00005-0.
[12] A.M.S. Jorge, K.K. Athira, M.B. Alves, R.L. Gardas, J.F.B. Pereira, Textile dyes effluents: a current scenario and the use of aqueous biphasic systems for the recovery of dyes, J. H2O Process Eng. 55 (2023) 104125, https://doi.org/10.1016/j.jwpe.2023.104125.
[13] M.G. Freire, Ionic-Liquid-Based Aqueous Biphasic Systems, Springer Berlin Heidelberg, Berlin, Heidelberg, 2016, https://doi.org/10.1007/978-3-662-52875-4.
[14] X. Lu, B. Wang, L. Zou, New aqueous two-phase system formed by piperazinium-based surface-active ionic liquid for extraction of dyes, J. Mol. Liq. 396 (2024) 124075, https://doi.org/10.1016/j.molliq.2024.124075.
[15] E. Atefi, R. Joshi, J.A. Mann, H. Tavana, Interfacial tension effect on cell partition in aqueous two-phase systems, ACS Appl. Mater. Interfaces 7 (2015) 21305–21314, https://doi.org/10.1021/acsami.5b05757.
[16] C. Fick, Z. Khan, S. Srivastava, Interfacial stabilization of aqueous two-phase systems: a review, Mater. Adv. 4 (2023) 4665–4678, https://doi.org/10.1039/D3MA00307H.
[17] M.G. Freire, J.F.B. Pereira, M. Francisco, H. Rodríguez, L.P.N. Rebelo, R.D. Rogers, J.A.P. Coutinho, Insight into the interactions that control the phase behaviour of new aqueous biphasic systems composed of polyethylene glycol polymers and ionic liquids, Chem. A Eur. J. 18 (2012) 1831–1839, https://doi.org/10.1002/chem.201101780.
[18] J.F.B. Pereira, L.P.N. Rebelo, R.D. Rogers, J.A.P. Coutinho, M.G. Freire, Combining ionic liquids and polyethylene glycols to boost the hydrophobic–hydrophilic range of aqueous biphasic systems, Phys. Chem. Chem. Phys. 15 (2013) 19580, https://doi.org/10.1039/c3cp53701c.
[19] J.F.B. Pereira, A. Magri, M.V. Quental, M. Gonzalez-Miquel, M.G. Freire, J.A. P. Coutinho, Alkaloids as alternative probes to characterize the relative hydrophobicity of aqueous biphasic systems, ACS Sustain Chem. Eng. 4 (2016) 1512–1520, https://doi.org/10.1021/acssuschemeng.5b01466.
[20] F.M. Maia, O. Rodríguez, E.A. Macedo, Relative hydrophobicity of equilibrium phases in biphasic systems (ionic liquid+H2O), J. Chem. Thermodyn. 48 (2012) 221–228, https://doi.org/10.1016/j.jct.2011.12.025.
[21] B.Yu Zaslavsky, L.M. Miheeva, S.V. Rogozhin, Parameterization of hydrophobic properties of aqueous polymeric biphasic systems and H2O-organic solvent systems, J. Chromatogr. A 212 (1981) 13–22, https://doi.org/10.1016/S0021-9673(00)80542-7.
[22] J.F.B. Pereira, K.A. Kurnia, O.A. Cojocaru, G. Gurau, L.P.N. Rebelo, R.D. Rogers, M. G. Freire, J.A.P. Coutinho, Molecular interactions in aqueous biphasic systems composed of polyethylene glycol and crystalline vs. Liquid cholinium-based salts, Phys. Chem. Chem. Phys. 16 (2014) 5723, https://doi.org/10.1039/c3cp54907k.
[23] U. Dorn, S. Enders, Heat of mixing and liquid–liquid-equilibrium of H2O + polypropylene glycol (PPG) with different molecular weights and H2O + propylene glycol dimethyl ether, Fluid Ph. Equilib. 424 (2016) 58–67, https://doi.org/10.1016/j.fluid.2015.10.003.
[24] R. Sadeghi, M. Maali, Toward an understanding of aqueous biphasic formation in polymer–polymer aqueous systems, Polymer 83 (2016) 1–11, https://doi.org/10.1016/j.polymer.2015.11.032.
[25] Z. Zhang, Polar and dispersive surface tension components of H2O-guanidinium chloride (Gdmcl) binary mixtures, Colloids Surf. A Physicochem. Eng. Asp. 676 (2023) 132223, https://doi.org/10.1016/j.colsurfa.2023.132223.
[26] J. Restolho, J.L. Mata, B. Saramago, On the interfacial behavior of ionic liquids: surface tensions and contact angles, J. Colloid Interface Sci. 340 (2009) 82–86, https://doi.org/10.1016/j.jcis.2009.08.013.
[27] R.J. Good, C.J. van Oss, The modern theory of contact angles and the hydrogen bond components of surface energies. Modern Approaches to Wettability, Springer US, Boston, MA, 1992, pp. 1–27, https://doi.org/10.1007/978-1-4899-1176-6_1.
[28] R.J. Good, Contact angle, wetting, and adhesion: a critical review, J. Adhes. Sci. Technol. 6 (1992) 1269–1302, https://doi.org/10.1163/156856192X00629.
[29] C.J. Van Oss, M.K. Chaudhury, R.J. Good, Interfacial Lifshitz-van der waals and polar interactions in macroscopic systems, Chem. Rev. 88 (1988) 927–941, https://doi.org/10.1021/cr00088a006.
[30] W.A. Zisman, Relation of the equilibrium contact angle to liquid and solid constitution. Advances in Chemistry, American Chemical Society, 1964, pp. 1–51, https://doi.org/10.1021/ba-1964-0043.ch001.
[31] D. Li, A.W. Neumann, Equation of state for interfacial tensions of solid-liquid systems, Adv. Colloid Interface Sci. 39 (1992) 299–345, https://doi.org/10.1016/0001-8686(92)80064-5.
[32] E. Moy, A.W. Neumann, Solid/liquid interfacial tensions from contact angle data and direct force measurements, J. Colloid Interface Sci. 119 (1987) 296–297, https://doi.org/10.1016/0021-9797(87)90273-6.
[33] J. Bergfreund, S. Siegenthaler, V. Lutz-Bueno, P. Bertsch, P. Fischer, Surfactant adsorption to different fluid interfaces, Langmuir 37 (2021) 6722–6727, https://doi.org/10.1021/acs.langmuir.1c00668.
[34] G.As Georgiev, S. Baluschev, P. Eftimov, M. Bacheva, K. Landfester, Addressing the apparent controversies between the contact angle-based models for estimation of surface free energy: a critical review, Colloids Interfaces 8 (2024) 62, https://doi.org/10.3390/colloids8060062.
[35] Z. Zhang, W. Wang, A.N. Korpacz, C.R. Dufour, Z.J. Weiland, C.R. Lambert, M. T. Timko, Binary liquid mixture contact-angle measurements for precise estimation of surface free energy, Langmuir 35 (2019) 12317–12325, https://doi.org/10.1021/acs.langmuir.9b01252.
[36] M. Gindl, G. Sinn, W. Gindl, A. Reiterer, S. Tschegg, A comparison of different methods to calculate the surface free energy of wood using contact angle measurements, Colloids Surf. A Physicochem. Eng. Asp. 181 (2001) 279–287, https://doi.org/10.1016/S0927-7757(00)00795-0.
[37] D.K. Owens, R.C. Wendt, Estimation of the surface free energy of polymers, J. Appl. Polym. Sci. 13 (1969) 1741–1747, https://doi.org/10.1002/app.1969.070130815.
[38] M.R. Almeida, H. Passos, M.M. Pereira, Á.S. Lima, J.A.P. Coutinho, M.G. Freire, Ionic liquids as additives to enhance the extraction of antioxidants in aqueous two-phase systems, Sep Purif. Technol. 128 (2014) 1–10, https://doi.org/10.1016/j.seppur.2014.03.004.
[39] T. Young, An essay on the cohesion of fluids, Philos. Trans. R. Soc. Lond. 1 (1832) 171–172, https://doi.org/10.1098/rspl.1800.0095.
[40] K. Song, J. Lee, S.-O. Choi, J. Kim, Interaction of surface energy components between solid and liquid on wettability, and its application to textile Anti-Wetting finish, Polymers 11 (2019) 498, https://doi.org/10.3390/polym11030498.
[41] Y. Wang, C.J. Hansen, C.-C. Wu, E.J. Robinette, A.M. Peterson, Effect of surface wettability on the interfacial adhesion of a thermosetting elastomer on glass, RSC Adv. 11 (2021) 31142–31151, https://doi.org/10.1039/D1RA05916E.
[42] H.-J. Choi, M.S. Kim, D. Ahn, S.Y. Yeo, S. Lee, Electrical percolation threshold of carbon black in a polymer matrix and its application to antistatic fibre, Sci. Rep. 9 (2019) 6338, https://doi.org/10.1038/s41598-019-42495-1.
[43] J. Sygusch, M. Rudolph, A contribution to wettability and wetting characterisation of ultrafine particles with varying shape and degree of hydrophobization, Appl. Surf. Sci. 566 (2021) 150725, https://doi.org/10.1016/j.apsusc.2021.150725.
[44] S. Hezaveh, S. Samanta, G. Milano, D. Roccatano, Molecular dynamics simulation study of solvent effects on conformation and dynamics of polyethylene oxide and polypropylene oxide chains in H2O and in common organic solvents, J. Chem. Phys. 136 (2012), https://doi.org/10.1063/1.3694736.
[45] H.Y. Erbil, Surface Chemistry of Solid and Liquid Interfaces, Wiley-Blackwell, 2006, https://doi.org/10.1002/9781444305401.
[46] A. Patra, A. Bandyopadhyay, S. Roy, J.A. Mondal, Origin of strong hydrogen bonding and preferred orientation of H2O at uncharged polyethylene glycol Polymer/H2O interface, J. Phys. Chem. Lett. 14 (2023) 11359–11366, https://doi.org/10.1021/acs.jpclett.3c03098.
[47] A.A. Oshiro, A.M.S. Jorge, V.C. Santos-Ebinuma, J.F.B. Pereira, Evaluation of ethanol-based aqueous two-phase systems performance for application in centrifugal partition chromatography (CPC), Sep Purif. Technol. 329 (2024) 125114, https://doi.org/10.1016/j.seppur.2023.125114.